The Econometrics Journal

Econometrics Journal (2023), volume **26**, pp. 444–466.
https://doi.org/10.1093/ectj/utad004

Disentangling the effect of measures, variants, and vaccines on SARS-CoV-2 infections in England: a dynamic intensity model

OTILIA BOLDEA[†], ADRIANA CORNEA-MADEIRA[‡] AND JOÃO MADEIRA[§]

[†]*Department of Econometrics and OR, Tilburg University, Warandelaan 2, 5000 LE Tilburg, The Netherlands.*
E-mail: o.boldea@uvt.nl

[‡]*ISEG - Universidade de Lisboa and CEMAPRE Rua do Quelhas 6, 1200-781 Lisboa, Portugal.*
E-mail: amadeira@iseg.ulisboa.pt

[§]*Department of Economics and BRU–Business Research Unit, ISCTE-University Institute of Lisbon, Av. das Forças Armadas, 1649-026 Lisboa, Portugal.*
E-mail: jarma2@iscte-iul.pt

First version received: 28 February 2022; final version accepted: 1 August 2022.

Summary: In this paper, we estimate the path of daily SARS-CoV-2 infections in England from the beginning of the pandemic until the end of 2021. We employ a dynamic intensity model, where the mean intensity conditional on the past depends both on past intensity of infections and past realized infections. The model parameters are time-varying, and we employ a multiplicative specification along with logistic transition functions to disentangle the time-varying effects of nonpharmaceutical policy interventions, of different variants, and of protection (waning) of vaccines/boosters. Our model results indicate that earlier interventions and vaccinations are key to containing an infection wave. We consider several scenarios that account for more infectious variants and different protection levels of vaccines/boosters. These scenarios suggest that, as vaccine protection wanes, containing a new wave in infections and an associated increase in hospitalizations in the near future may require further booster campaigns and/or nonpharmaceutical interventions.

Keywords: *COVID-19*, *Bayesian Hamiltonian Monte Carlo*, *NPI*, *vaccines*, *booster*, *variants of concern*, *Omicron*.

JEL codes: *C11*, *C51*, *C63*, *I18*, *H12*.

1. INTRODUCTION

In this paper, we use data on SARS-CoV-2 infections in England to estimate a time series model, where the intensity of infections depends on both the level and intensity of past infections. We use this model to quantify the impact of the Omicron BA.1/BA.2 sub-variants and of the waning of immunity from vaccines/boosters on the COVID-19 epidemic in England, and to assess the timing and intensity of nonpharmaceutical interventions (NPIs) and further booster campaigns that may still be needed to curb future infection waves. Our model results suggest that further infections waves still require interventions.

There are two main challenges when fitting a model of COVID-19 to the data. First, the true number of cases is not observed and the ratio of unreported to reported cases varies over time, due to both changes in testing capacity and in testing behaviour. Some econometric studies ignore unreported cases and model only reported cases (Lee et al. 2021, Liu et al. 2021, Jiang et al. 2023, and Khismatullina and Vogt, 2023); this can lead to inconsistent parameter estimates or to serious mid- and long-term forecasting errors, depending on the goal of the study (Korolev, 2021). Other studies employ various strategies to identify the share of unreported cases: Li et al. (2020) and Hortaçsu et al. (2021) identify the unreported cases through their mobility across regions; Rozhnova et al. (2021), Toulis (2021), Viana et al. (2021), and Arias et al. (2023), use random sample serology tests; Gourieroux and Jasiak (2023) use parametric time-varying transition probabilities, and Sonabend et al. (2021) use random tests in the population. We use the last identification strategy, as England runs a bi-weekly random sample population survey based on polymerase chain reaction (PCR) tests, from which we construct a time-varying ratio of total to reported cases, and apply it to (delayed) daily reported cases to approximate the total daily cases.

The second main challenge is model complexity. Most of the large-scale stochastic epidemiological modelling papers that address the effectiveness of policy interventions compartmentalize the population into susceptible, exposed, infected, recovered, and possibly other states such as hospitalizations or deaths. These models are necessarily complex over longer periods of time, because, for example, only modelling infections in vaccinated or waned vaccinated typically require introducing another set of compartments for each, and therefore more unobservables (see, e.g., Sonabend et al., 2021, and the citations therein). Because data on each infection type is typically not available at higher frequency, several parameters in these models are unidentified and require calibration. With these additional calibrations, these models can be estimated by Bayesian filtering methods, although, due to nonlinearity compound with several (unobserved) state variables and many parameters, their estimation can pose substantial computational challenges.[1]

To reduce model complexity while allowing for vaccination and its waning, we propose a different approach, where the population is not compartmentalized, and the effect of seasonality, vaccination, and waning enters the model parameters multiplicatively to the effect of variants of concern and that of NPIs. To that end, we employ a dynamic intensity model with time-varying parameters, where infections are assumed to follow a negative binomial distribution to allow for overdispersion. This model is akin to integer generalized autoregressive conditional heteroskedasticity (INGARCH) models, but instead of modelling variance clustering, it models intensity clustering: when the intensity of the infection process is high, it stays high for a while and it is reinforced by the level of past infections.[2]

The model parameters vary based on individuals' behaviour as a result of NPIs. We estimate both the timing and the magnitude of the behavioural response following NPIs in a similar fashion to Rozhnova et al. (2021) and Viana et al. (2021). The parameters also vary with vaccination,

[1] See, e.g., the Supplementary Material in Sonabend et al. (2021), which describes how they estimate an age-structured, regional, multiple vaccine type, multiple variant model.

[2] The dynamic INGARCH model was also used by Agosto and Giudici (2020), Roy and Karmakar (2021), and Giudici et al. (2023) to model COVID-19 in the USA and Italy, although without accounting for overdispersion. The first study assumes stationarity and constant parameters, therefore not accounting for NPIs. The second study models NPIs nonparametrically, with Bayesian B-Splines, which makes it difficult to establish which periods relate to a particular NPI. Giudici et al. (2023) use the Oxford COVID-19 Government Response Tracker to create NPI variables, which are then included as exogenous variables in the model, but this approach ignores endogeneity of individuals' responses to NPIs. Unlike our study, all three studies mentioned only use reported infections and do not account for vaccination, waning of vaccines, or variants of concern.

and we estimate the intensity reduction from vaccination based on the vaccine schedule and the total infections. This allows us to combine different administered vaccines into a single vaccine intensity reduction parameter without requiring separate data on infections of vaccinated and nonvaccinated individuals, data which is not available at daily frequency. The parameters also vary with variants of concern, and we estimate the timing and the effect of these variants in a similar fashion to Viana et al. (2021). The seasonality cannot be identified separately and is calibrated based on previous studies.

The advantage of our model over more complex models is that it can be estimated relatively quickly, and therefore can be used in real-time to inform policy makers on the interventions needed and their timing, depending on new variants and (waning) effects of boosters. The disadvantage compared to more complex epidemiology models is that we did not separately account for temporary protection due to a previous infection. However, since a large fraction of individuals are susceptible to Omicron, regardless of their previous infection status (Reynolds et al., 2022), our model provides a good approximation to the path of infections in the near future.

As the infection data is not stationary over long periods, we estimate the model via Bayesian Hamiltonian Monte Carlo methods. Disentangling the effect of vaccines and boosters from those of variants and NPIs allows us to employ counterfactuals and provide scenarios for the future six months, both using NPIs and further booster campaigns.

Our counterfactuals show that the timing of NPIs and of vaccines and boosters is key in curbing infections waves. We find that the recent Omicron wave could have been substantially mitigated by earlier timing and faster speed of vaccine and booster schedules, or two weeks of lockdown in mid-December 2021. Our scenarios show that another wave is likely due to booster waning, and its occurrence depends on a range of factors. First, on the transmissibility of the Omicron sub-variants: if its intensity increase relative to Omicron BA.1 is 10% or larger, a new wave occurs earlier. Second, on the choice of NPIs: maintaining semi-lockdown restrictions from mid-December of 2021, in the absence of a new variant, may delay the next infection wave to the summer. Third, on the effectiveness of boosters: if the booster intensity reduction is sufficiently high, under some scenarios another infection wave is substantially delayed.

In the Online Appendix we also examine the implications these scenarios have for new hospital admissions. Our projected hospital admissions track well observed hospital admissions, and we find that new hospitalizations rise steeply, shortly after the start of another infection wave.

The rest of the paper is organized as follows. Section 2 describes the model. Subsection 3.1 describes the data. Subsection 3.2 contains estimation results. Subsection 3.3 presents the counterfactual analysis, and Subsection 3.4 provides projections of daily infections for the spring and summer of 2022. Section 4 concludes. The Online Appendix provides a further discussion of behavioural aspects implied by our model and results, robustness checks related to the uncertainty in the constructed total case data, plots of parameter posterior distributions along with parameter identification results obtained by simulation, additional counterfactuals and scenarios, and implications of some scenarios for new hospital admissions.

2. MODEL

We model the daily total COVID-19 cases (reported and unreported), y_t, as a negative binomial conditional response model. When exposed to the virus, individuals are typically heterogeneous

in terms of their latent period (duration from exposure to becoming infectious) and their infectious period/transmission of disease. A common and parsimonious way to account for this heterogeneity when aggregating across individuals is to use the negative binomial distribution, which is a Gamma mixture of Poisson distributions, where the Gamma distribution models heterogeneous delays in becoming exposed and infectious—see, e.g., Wearing et al. (2005) and Lloyd-Smith et al. (2005). Therefore, the conditional response model is:

$$y_t|\mathcal{F}_{t-1} \sim \text{NegBinomial}(\lambda_t, \phi). \tag{2.1}$$

The probability distribution function is given by

$$\binom{y+\phi-1}{y}\left(\frac{\lambda_t}{\lambda_t+\phi}\right)^y\left(\frac{\phi}{\lambda_t+\phi}\right)^\phi,$$

with $\lambda_t \in \mathbb{R}^+$, $\phi \in \mathbb{R}^+$, $y \in \mathbb{N}$.[3] The mean and the variance are given by $E[y_t|\mathcal{F}_{t-1}] = \lambda_t$ and $Var[y_t|\mathcal{F}_{t-1}] = \lambda_t + \lambda_t^2/\phi$, where λ_t^2/ϕ is the additional variance above the mean λ_t, $\mathcal{F}_{t-1} = \{y_{t-1}, \lambda_{t-1}, y_{t-2}, \lambda_{t-2}, \ldots\}$, and

$$\lambda_t = \lambda_t^{\text{npi}}\, s_t\, \text{voc}_t\, \text{vir}_t\, \text{bir}_t, \tag{2.2}$$

where λ_t^{npi} is the daily intensity of infections due to NPIs (either restrictions or relaxation of restrictions), s_t is seasonality, and voc_t, vir_t, and bir_t are changes in intensity due to variants of concern, vaccines, and boosters. To account for the seasonal pattern of SARS-CoV-2 (by which transmission is lower in summer and higher in winter), we define the sinusoidal function s_t (Sonabend et al., 2021, Supplementary Material, p. 44):

$$s_t = 1 + 0.1\cos(2\pi(t - t^*)/365.25),$$

where t^* is 1 January (due to coldest weather).

To account for the increase in intensity due to variants of concern, we define:

$$\begin{aligned}\text{voc}_t = {} & (1 - g_{\alpha,t}) + (1+\rho_\alpha)g_{\alpha,t}(1-g_{\delta,t}) + (1+\rho_\alpha)(1+\rho_\delta)g_{\delta,t}(1-g_{o,t}) \\ & + (1+\rho_\alpha)(1+\rho_\delta)(1+\rho_o)g_{o,t},\end{aligned}$$

where the parameters ρ_α, ρ_δ, and ρ_o represent the relative intensity increase of the Alpha, Delta, and Omicron BA.1 variants that became dominant in England in January 2021, June 2021, and December 2021, respectively. The intensity increase as the new variants take over is described using the logistic functions:

$$g_{j,t} = \frac{1}{1+\exp(-\kappa_j(t - t_j^*))}, \tag{2.3}$$

where $j = \alpha, \delta, o$ are the variants of concern, κ_j is the steepness of the logistic function, and t_j^* is the midpoint of the logistic function. The functions $g_{j,t}$ can be interpreted as probabilities of contracting the new variant, which increase over time, while ρ_j can be interpreted as the relative intensity increase when the new variant completely takes over. Therefore, as described

[3] We chose this alternative formulation of the negative binomial distribution to emphasize that we are modelling the dynamics in the conditional mean λ_t. If, instead, we use the formulation $y_t \sim \text{NegBinomial}(r, p_t)$, where y_t is the number of failures that occurred, given r successes (and p_t is the probability of success), then $\phi = r$ and $\lambda_t = \frac{1-p_t}{p_t}r$, and one can calculate from λ_t the implied odds ratio $\frac{1-p_t}{p_t}$.

in Subsection 3.1, we fitted the logistic functions (2.3) to external gene sequencing data as in Viana et al. (2021) and Hansen (2022), while ρ_j is estimated directly from fitting infection data.[4]

The effect of vaccinations and boosters and their waning is modelled as:

$$\text{vir}_t = (1 - g_{v,t}) + (1 - \text{vir}\ w_{v,t})g_{v,t},$$
$$\text{bir}_t = (1 - g_{b,t}) + (1 - \text{bir}\ w_{b,t})g_{b,t},$$

where vir_t and bir_t describe the vaccine and booster-induced intensity reduction. If there are no vaccinated individuals, vir_t and bir_t are equal to 1. As more vaccines are administered, vir_t and bir_t decrease to $(1 - \text{vir}\ w_{v,t})g_{v,t}$ and $(1 - \text{bir}\ w_{b,t})g_{b,t}$, respectively, where 'vir' is the vaccine (two doses) intensity reduction parameter and 'bir' is the booster intensity reduction parameter. The transition from no vaccination to vaccination is described by the logistic functions $g_{v,t}$ and $g_{b,t}$:

$$g_{j,t} = \frac{c}{1 + \exp(-h_j(t - t_j^{\perp}))}, \tag{2.4}$$

with $j = v, b$, where h_j is the steepness and $t_j^{\perp}$ is the midpoint of the transition function. We assume $c = 0.7$ (the fraction of the total population of England that had the second dose of the vaccine by the beginning of January 2022 when our sample ends). The logistic transition function for the vaccine and booster uptake $g_{v,t}$ and $g_{b,t}$ are fitted to the total share of vaccinations and boosters administered in the population, as explained in Subsection 3.1. Following Keeling et al. (2021), we introduce waning of vaccine protection against infection through the exponential function:

$$w_{j,t} = \begin{cases} \exp(-\frac{t-t^+}{180}), & \text{if } t > t^+, \\ 1, & \text{if } t^+ \leq t, \end{cases} \tag{2.5}$$

where $j = v, b$. For the estimation, we assume that the waning of vaccines starts on 28 June 2021, hence $t^+ = 28$ June 2021 (six months after the first second-dose vaccine was administered on 29 December 2020). For the booster, we do not assume waning in the estimation since our estimation ends on 24 December 2021 (three months after the first dose of the booster was administered on 16 September 2021). However, in the counterfactuals (Subsection 3.3) and scenarios (Subsection 3.4) we assume that the boosters wane after five months, while the results for four and six months are relegated to the Online Appendix.

[4] To motivate this choice further, note that the probabilities $g_{j,t}$ are unlikely to be identified within the dynamic intensity model separately from the time-varying effect of vaccinations and NPIs. Additionally, Götz et al. (2021) show that if the number of susceptible individuals is equal to the population in an SIR (susceptible-infected-recovered) model with two virus strains, then $g_{j,t}$ fitted to the share of the new variant in all cases within a period can be used to approximate the transition in infectiousness from the old variant to the new one. Hansen (2022) shows this as well, without using an SIR model. In both papers, the κ_j parameter directly relates to relative infectiousness of the new variant. We instead estimate ρ_α, ρ_δ, and ρ_o directly within the dynamic intensity model, following Viana et al. (2021), and therefore assuming that we reach an average new intensity when the transition is completed.

Table 1. NPIs transition functions.

NPI transitions	Meaning
$f_{1,t}$	First lockdown in 2020 to relaxation measures in the summer 2020
$f_{2,t}$	Relaxation measures in the summer 2020 to second lockdown in November 2020
$f_{3,t}$	Second lockdown to some relaxation measures before Christmas 2021
$f_{4,t}$	Relaxation measures before Christmas 2020 to third lockdown in January 2021
$f_{5,t}$	Lockdown in January 2021 to relaxation measures in spring 2021
$f_{6,t}$	Further relaxation measures and big gatherings (the Euro 2020 football tournament end of June to beginning of July 2021)
$f_{7,t}$	No big crowded events (July 2021, after the end of the Euro 2020 tournament)
$f_{8,t}$	Transition to a period with full relaxation (no restrictions) including Schools/universities opening (from July 2021 to October 2021)
$f_{9,t}$	Transition from school opening to school holiday (after late October 2021)

We specify λ_t^{npi} as:

$$\begin{aligned}
\lambda_t^{\text{npi}} &= \theta_t^{\text{npi}} y_{t-1} + \beta_t^{\text{npi}} \lambda_{t-1}^{\text{npi}}, \\
\theta_t^{\text{npi}} &= \theta_0(1 - f_{1,t}) + \sum_{i=1}^{8} \theta_i f_{i,t}(1 - f_{i+1,t}) + \theta_9 f_{9,t}, \\
\beta_t^{\text{npi}} &= \beta_0(1 - f_{1,t}) + \sum_{i=1}^{8} \beta_i f_{i,t}(1 - f_{i+1,t}) + \beta_9 f_{9,t}.
\end{aligned} \tag{2.6}$$

As can be seen from (2.6), λ_t^{npi} is triggered by the previous day infections (y_{t-1}) and previous day intensity ($\lambda_{t-1}^{\text{npi}}$). The parameters, $\theta_i \geq 0$ and $\beta_i \geq 0$, $i = 0, \ldots, 9$ associated with y_{t-1} and $\lambda_{t-1}^{\text{npi}}$ change in each NPI regime by γ_i and ω_i, respectively: $\theta_i = \theta_{i-1} + (-1)^i \gamma_i$, $\beta_i = \beta_{i-1} + (-1)^i \omega_i$ $i = 1, \ldots, 9$, through the following logistic transition functions which are estimated within the model:

$$f_{i,t} = \frac{1}{1 + \exp(-k_i(t - t_i^+))}, \quad i = 1, \ldots, 9, \tag{2.7}$$

where k_i describe the speed at which restrictions or relaxation measures are taken up by individuals, and t_i^+ describe the mid-time of the take-up of a restriction/relaxation. The correspondence between each regime and NPIs is described in Table 1, where only the last regime does not refer to an NPI, but to an transition to school holidays; nevertheless, we refer to it for simplicity as an NPI regime.

We now discuss the model assumptions embedded in the specification of λ_t^{npi}. First, we assume that NPIs are effective in changing behaviour, by setting $\omega_i, \gamma_i \neq 0$, and, for counterfactuals and projections, we also assume that this behavioural change would not have happened in the absence of the NPIs we modelled. Second, we impose the direction of this behavioural change following each NPI, by assuming the changes in θ_i, β_i are $(-1)^i \omega_i, (-1)^i \gamma_i$. This means that lockdowns decrease θ_i, β_i and relaxations increase θ_i, β_i, except when relaxations are very gradual, as in regime 1 in Table 1. Third, the logistic functions $f_{i,t}$ approximate the timing and speed of individuals' behavioural adjustment following NPIs, similarly to Rozhnova et al. (2021) and Viana et al. (2021). As a new NPI is implemented, the average number of contacts, and therefore

also θ_i, β_i, change gradually to a new level, and the timing, speed, and magnitude of this change is influenced by behaviour, which is allowed to adjust ahead or after measures are implemented, and differently in each regime in the sample. Fourth, we did not explicitly model temporary protection from a previous infection, along with its waning over time.[5]

3. RESULTS

3.1. Data and estimation method

Data on variants of concern. We obtained the weekly percentage of COVID-19 positive cases by gene pattern and Cycle threshold (Ct) value from the Office for National Statistics (ONS) (2022a) Coronavirus (COVID-19) Infection Survey from England, and we linearly interpolated them to obtain the daily percentage of COVID-19 positive cases. For the Alpha variant we used gene sequencing data from 3 December 2020 until 10 January 2021. The Alpha variant was identified if the ORF1ab and N genes were present. For the Delta variant we used gene sequencing data between 26 April 2021 and 6 December 2021. The Delta variant was identified if ORF1ab, N and S genes were present. For the Omicron BA.1 variant we used gene sequencing data between 29 November 2021 and 3 January 2022. The Omicron BA.1 variant was identified because of the absence of the S-gene in combination with the presence of the ORF1ab and N genes. The logistic functions (2.3) were fitted to the daily percentage of COVID-19 positive cases by gene.

Data on vaccines and boosters. We used daily observations for England from the official COVID-19 UK dashboard (UK Health Security Agency, 2022) on new people vaccinated with the second dose and new people receiving a booster dose (from December 29, 2021 until January 13, 2022, and from September 16, 2021 until January 13, 2022, respectively). The logistic functions (2.4) were fitted to the daily cumulative fraction of people vaccinated with the second dose and receiving the booster.

Constructed Daily Cases. For the model in (2.2), our data is from 3 May 2020 until 22 January 2022, a total of $N = 630$ daily infections.[6] We estimate (2.2) until 24 December, and use the data from 25 December 2021 until 22 January 2022 to assess the out of sample fit of the model's projections (in Subsection 3.4). The daily infections y_t in (2.6) refer to the reported and unreported cases, $y_t = y_t^r + y_t^u$. For the reported daily infections y_t^r, we used new cases by specimen date obtained from the official COVID-19 UK dashboard (Office for National Statistics, 2022b). To approximate the total daily infections, we proceeded as follows. Denote by $Y_1^r = \sum_{t=t_1}^{t_{14}} y_t^r$ the reported cases by specimen date for the period 3–16 May 2020, ..., $Y_{45}^r = \sum_{t=t_{617}}^{t_{630}} y_t^r$ the reported cases by specimen date for the period 9–22 January 2022. The reported cases are considered to be reported with a delay of two days since the onset of the symptoms (Casey-

[5] In principle, this could be modelled by an upper-truncated negative binomial model, where the upper truncation is time-varying and depends on the number of individuals susceptible in the population at a given time. This would require further assumptions about the duration of protection from an infection and its waning. But these may be differential among the vaccinated and nonvaccinated, and our model does not distinguish between infection types. Therefore, in our model, temporary protection and its waning are partly absorbed by the parameters θ_i and β_i. To see why, recall that the parameter β_i models intensity clustering, in a similar fashion to volatility clustering in GARCH models: everything else constant, if this parameter is low (for example because many individuals are still protected from a new infection by a previous infection), then a wave may die out quicker, and if it is high, it may persists for longer. The parameter θ_i is also tied to the average number of contacts in the population, and therefore can also be influenced by temporary protection and its waning. This is a drawback relative to more sophisticated epidemiological models, and we take this drawback into account when interpreting the results in the next sections.

[6] The first observation for the PCR test surveillance in random samples of the population is 3 May 2020.

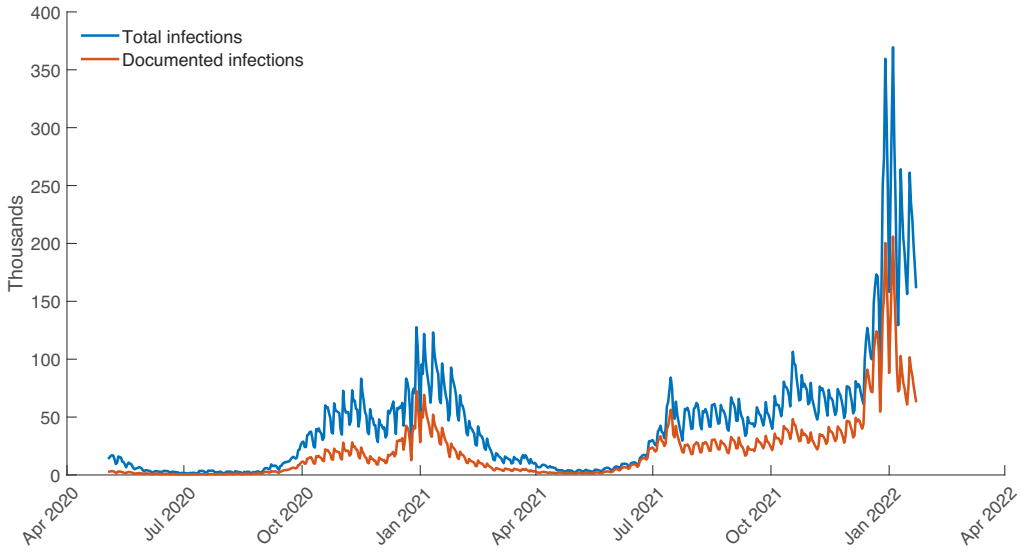

Figure 1. Total infections and reported infections between May 3, 2020 until January 22, 2022 in England.

Bryars et al., 2021). Denote by $Y_1 = \sum_{t=t_1-2}^{t_{12}} y_t$ the total infections for the period 1–14 May 2020, . . ., $Y_{45} = \sum_{t=615}^{t_{628}} y_t$ the total infections for the period 7–20 January 2022. From the ONS Infection Survey (Office for National Statistics, 2022c) we have the estimated percentage (say p_j) of the population that had COVID-19 for a time period of 14 days. Then, $Y_j = p_j \times 56550138$, where 56550138 is the population in England (based on the ONS mid-year population estimates, June 2020). We calculate $r_j = Y_j / Y_j^r$, the ratio of total to reported infections in the two-week period j, $j = 1, \ldots, 45$. To calculate the daily total cases we assume the daily ratio of total to reported infections within a 14-day period is equal to the two-week ratio corresponding to that 14-day period. Let $\tilde{r}_t$ denote the daily ratio of total to reported cases; then the total cases are $y_t = \tilde{r}_t y_j^r$. Note that we constructed daily data because some of the NPIs transition functions are too short to use bi-weekly data, and could not have been estimated otherwise.

The total and reported new cases are shown in Figure 1. The divergence between the two series is highest in times of high incidence, possibly due to limits to testing capacity, but also possibly due to testing behaviour, suggesting that correcting for unreported cases is essential to remove the time-varying sample selection bias in reported cases.[7]

Estimation. Because total cases are not stationary, we use Bayesian estimation with Hamiltonian Monte Carlo (HMC) methods, implemented in R Stan, and for simplicity we also did so for stationary data such as the share of new variants or cumulative vaccine/boosters uptake. Neal (2011) and Fernández-Villaverde and Guerrón-Quintana (2021) provide a description of the HMC, and highlight its computational efficiency relative to traditional Markov Chain Monte Carlo (MCMC) methods, due to exploiting information from the gradient of the posterior, which reduces the correlation between successive parameter values in the Markov chain, and therefore ensures that the Markov chain converges much faster than in MCMC.

[7] The Online Appendix Section S1, Figure S1, shows the time-varying ratio of total to reported cases.

Table 2. Prior distributions of the parameters in the model.

Parameter	Prior	Description
θ_0	LogN(0, 1)	Vague prior (infections data)
γ_i	LogN(0, 1)	$i = 1, \ldots, 9$, vague prior (infections data)
β_0	LogN(0, 1)	Vague prior (infections data)
ω_i	LogN(0, 1)	$i = 1, \ldots, 9$, vague prior (infections data)
ρ_α	LogN(0, 0.5)	Vague prior for Alpha (infections data)
ρ_δ	LogN(0, 1)	Larger scale than for Alpha (infections data)
ρ_o	LogN(2, 2)	Larger scale than for Delta (infections data)
vir	Beta(5, 2)	Gives more probability mass to values larger than 0.5 (infections data)
bir	Beta(5, 2)	Gives more probability mass to values larger than 0.5 (infections data)
k_i	Exp(1)	$i = 1, \ldots, 9$ (infections data)
t_1^+	N(35,7)	35 = 6 June 2020, relaxation in the summer 2020 (infections data)
t_2^+	N(140,7)	140 = 19 September 2020, transition to the second lockdown in November 2020 (infections data)
t_3^+	N(200,7)	200 = 18 November 2020, transition from the lockdown in November 2020 to relaxation (infections data)
t_4^+	N(230,7)	230 = 18 December 2020, transition from relaxation to lockdown in January 2021 (infections data)
t_5^+	N(270,7)	270 = 27 January 2021, transition from the lockdown in January 2021 to relaxation (infections data)
t_6^+	N(425,7)	425 = 1 July 2021, transition to large crowds events (Euro 2020) (infections data)
t_7^+	N(440,7)	440 = 16 July 2021 transition to no large crowed events (infections data)
t_8^+	N(515,7)	515 = 29 September 2021 transition to a period with full relaxation and schools/universities opening (infections data)
t_9^+	N(555,7)	555 = 8 November 2021, transition from school opening to school holiday (infections data)
ϕ	LogN(0,1)	Vague prior (infections data)
κ_i	Exp(1)	As in Rozhnova et al. (2021), $\kappa_i = 1$ means lift-up $\sim$ 6 days ($i = \alpha, \delta, o$) (gene data)
t_α^*	N(10,7)	10 = 12 December 2020, around the date when Alpha became dominant (gene data)
t_δ^*	N(10,7)	10 = 26 April 2021, around the date that Delta emerged (gene data)
t_o^*	N(17,7)	17 = 15 December 2021, around the date Omicron became dominant (gene data)
σ_j	LogN(0,1)	Vague prior, $j = \alpha, \delta, o, v, b$ (gene/vaccination/booster data)
h_i	Exp(1)	$i = v, b$ (vaccination/booster data)
$t_v^\perp$	N(190,7)	190 = 6 July 2021, around the date when 50% of the population had the vaccine (2nd dose) (vaccination data)
$t_b^\perp$	N(106,7)	106 = 12 December 2021, around the date 50% of the population had the booster (booster data)

Denoting by $x_{j,t}$ the daily percentage of COVID-19 positive cases due to the new variant or the daily cumulated vaccine/booster uptake, we assumed $x_{j,t} \sim N(g_{j,t}, \sigma_j^2)$, where $g_{j,t}$ is given by (2.3) (with $j = \alpha, \delta, o$) or (2.4) (with $j = v, b$). Table 2 lists the priors for all parameters—whether they are estimated using sequenced gene data, vaccine data, or infections—and motivates their choice.

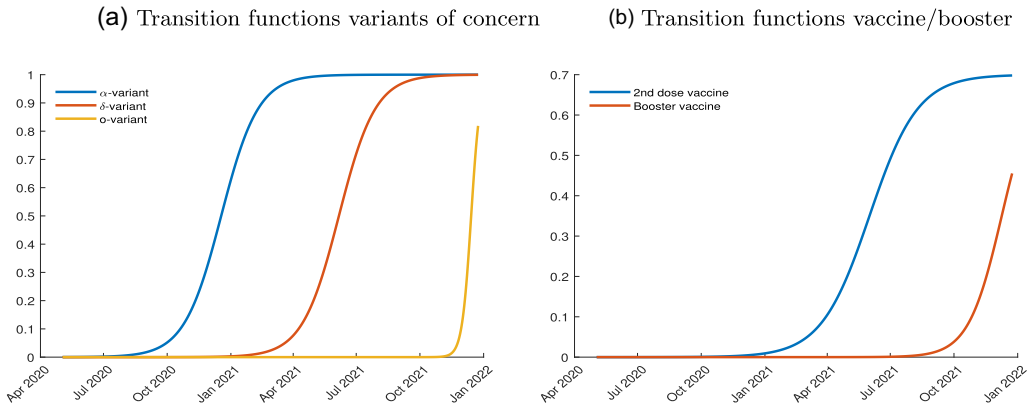

Figure 2. (a) Transition functions variants of concern (b) Transition functions vaccine/booster.

3.2. Posterior estimates

The transition functions for sequenced gene data and vaccination are shown in Figure 2 a and b.

The estimated steepness of the transition functions based on sequenced gene data is the highest for the Omicron BA.1 variant, 0.1508, while the steepness of transition function for the Delta variant, 0.0377, is slightly higher than for the Alpha variant, which is 0.0372. The estimated transition functions for the vaccines and boosters from the vaccination data show that the uptake of the booster is faster than the uptake of the vaccine second dose.

The median from the posterior predictive distribution, is plotted in Figure 3.[8] We can see from this figure that the discrepancies between the simulated data and real data are small.[9]

The rest of the parameters are estimated within the dynamic intensity model. The posterior medians along with their 90% credible intervals are listed in Table 3.[10] As can be seen from Table 3, the Alpha, Delta, and Omicron BA.1 variants result in 26%, 81%, and 41% higher relative intensity. The vaccine intensity reduction parameter estimates 'vir' and 'bir' are 49% and 69%, respectively.[11] The posterior medians for steepness of the transition functions in the regimes 8 and 9 (since the full relaxation in the summer 2021) are the highest (1.33 and 1.22, respectively). The overdispersion parameter estimate is large, showing that a model without overdispersion would fit the data poorly.

[8] We perform a posterior predictive check by simulating new replicated data from the posterior predictive distribution (the distribution over new observations given previous observations), see Gelman et al. (2020). We obtained 4,000 draws from the posterior predictive distribution and in Figure 3 we plot the median of these draws.

[9] In our framework we implicitly also model the $Var[y_t|\mathcal{F}_{t-1}] = \lambda_t + \lambda_t^2/\phi$ because of ϕ. We fit well the overall movement of $\widehat{Var}[y_t|\mathcal{F}_{t-1}]$ (obtained by plugging in the posterior medians from Table 3 below), but we overpredict the size of the deviations, which may be a drawback of the negative binomial.

[10] Note that in the paper, we only use the total case data as constructed in the previous section. However, the ONS survey (Office for National Statistics, 2022c) also reports 95% credible intervals to adjust for residual nonrepresentativeness in terms of age, sex, and region–Pouwels et al. (2021). In the Online Appendix Section S4 we report the results of our analysis with data constructed based on the 95% lower and upper credible intervals limits of the ONS survey, showing that our results are very robust to this measured uncertainty in the data. However, there may be other unobserved sources of selection bias in the survey, which we cannot control for and may bias our results.

[11] We stress here that 'vi' and 'bir' cannot be interpreted as vaccine and booster effectiveness against infection, as this is a term usually reserved for comparing vaccinated with nonvaccinated in a controlled setting.

Table 3. Posterior medians.

	Parameter	Posterior median	90% credible interval
Parameter associated with y_{t-1}	θ_0	0.94	[0.80, 1.16]
Parameter associated with y_{t-1} in regime 1	γ_1	0.06	[0.02, 0.29]
Parameter associated with y_{t-1} in regime 2	γ_2	0.03	[0.01, 0.06]
Parameter associated with y_{t-1} in regime 3	γ_3	0.44	[0.22, 0.71]
Parameter associated with y_{t-1} in regime 4	γ_4	0.20	[0.06, 0.46]
Parameter associated with y_{t-1} in regime 5	γ_5	0.05	[0.02, 0.10]
Parameter associated with y_{t-1} in regime 6	γ_6	0.10	[0.04, 0.20]
Parameter associated with y_{t-1} in regime 7	γ_7	0.17	[0.08, 0.30]
Parameter associated with y_{t-1} in regime 8	γ_8	0.10	[0.03, 0.24]
Parameter associated with y_{t-1} in regime 9	γ_9	0.14	[0.06, 0.28]
Parameter associated with λ_{t-1}	β_0	0.24	[0.12, 0.51]
Parameter associated with λ_{t-1} in regime 1	ω_1	0.05	[0.02, 0.28]
Parameter associated with λ_{t-1} in regime 2	ω_2	0.03	[0.01, 0.06]
Parameter associated with λ_{t-1} in regime 3	ω_3	0.15	[0.06, 0.29]
Parameter associated with λ_{t-1} in regime 4	ω_4	0.14	[0.06, 0.23]
Parameter associated with λ_{t-1} in regime 5	ω_5	0.06	[0.03, 0.12]
Parameter associated with λ_{t-1} in regime 6	ω_6	0.07	[0.03, 0.16]
Parameter associated with λ_{t-1} in regime 7	ω_7	0.17	[0.09, 0.28]
Parameter associated with λ_{t-1} in regime 8	ω_8	0.09	[0.04, 0.21]
Parameter associated with λ_{t-1} in regime 9	ω_9	0.09	[0.04, 0.20]
Intensity increase Alpha (relative to wild-type)	ρ_α	0.26	[0.15, 0.43]
Intensity increase Delta (relative to Alpha)	ρ_δ	0.81	[0.44, 1.34]
Intensity increase Omicron BA.1 (relative to Delta)	ρ_o	0.41	[0.10, 0.76]
Vaccine intensity reduction	vir	0.49	[0.22, 0.81]
Booster intensity reduction	bir	0.69	[0.38, 0.92]
Steepness NPI transition function regime 1	k_1	0.63	[0.12, 2.93]
Steepness NPI transition function regime 2	k_2	0.66	[0.12, 2.96]
Steepness NPI transition function regime 3	k_3	0.11	[0.10, 0.14]
Steepness NPI transition function regime 4	k_4	0.17	[0.11, 0.62]
Steepness NPI transition function regime 5	k_5	0.54	[0.12, 2.75]
Steepness NPI transition function regime 6	k_6	0.81	[0.13, 3.15]
Steepness NPI transition function regime 7	k_7	0.12	[0.10, 0.82]
Steepness NPI transition function regime 8	k_8	1.33	[0.35, 3.75]
Steepness NPI transition function regime 9	k_9	1.22	[0.22, 3.46]
Mid-time NPI transition function regime 1	t_1^+	25.50	[1.70, 43.75]
Mid-time NPI transition function regime 2	t_2^+	140.70	[128.17, 153.50]
Mid-time NPI transition function regime 3	t_3^+	201.38	[199.20, 206.56]
Mid-time NPI transition function regime 4	t_4^+	217.34	[212.59, 227.90]
Mid-time NPI transition function regime 5	t_5^+	260.72	[256.34, 271.44]
Mid-time NPI transition function regime 6	t_6^+	426.72	[414.96, 434.92]
Mid-time NPI transition function regime 7	t_7^+	441.96	[440.14, 447.71]
Mid-time NPI transition function regime 8	t_8^+	532.02	[519.98, 532.94]
Mid-time NPI transition function regime 9	t_9^+	535.63	[535.04, 542.43]

Table 3. Continued

	Parameter	Posterior median	90% credible interval
Overdispersion parameter	ϕ	18.60	[16.74, 20.56]
Steepness transition function Alpha	κ_α	0.0372	[0.0316, 0.0429]
Steepness transition function Delta	κ_δ	0.0377	[0.0331, 0.0433]
Steepness transition function Omicron BA.1	κ_o	0.1508	[0.1186, 0.1880]
Mid-time transition function Alpha	t^*_α	14.67	[12.90, 16.23]
Mid-time transition function Delta	t^*_δ	41.78	[39.65, 43.85]
Mid-time transition function Omicron BA.1	t^*_o	16.44	[15.20, 17.74]
Steepness transition function vaccines second dose	h_v	0.0285	[0.0279, 0.0291]
Standard deviation $N(g_{\alpha,t}, \sigma^2_\alpha)$	σ_α	0.0533	[0.0441, 0.0658]
Standard deviation $N(g_{\delta,t}, \sigma^2_\delta)$	σ_δ	0.0988	[0.0915, 0.1072]
Standard deviation $N(g_{o,t}, \sigma^2_o)$	σ_o	0.1551	[0.1216, 0.2023]
Standard deviation $N(g_{v,t}, \sigma^2_v)$	σ_v	0.0909	[0.0856, 0.0967]
Standard deviation $N(g_{b,t}, \sigma^2_b)$	σ_b	0.0153	[0.0138, 0.0172]
Steepness transition function booster	h_b	0.0414	[0.0406, 0.0422]
Mid-time transition function vaccine second dose	$t^\perp_v$	155.32	[154.49, 156.16]
Mid-time transition function booster	$t^\perp_b$	85.47	[84.98, 85.94]

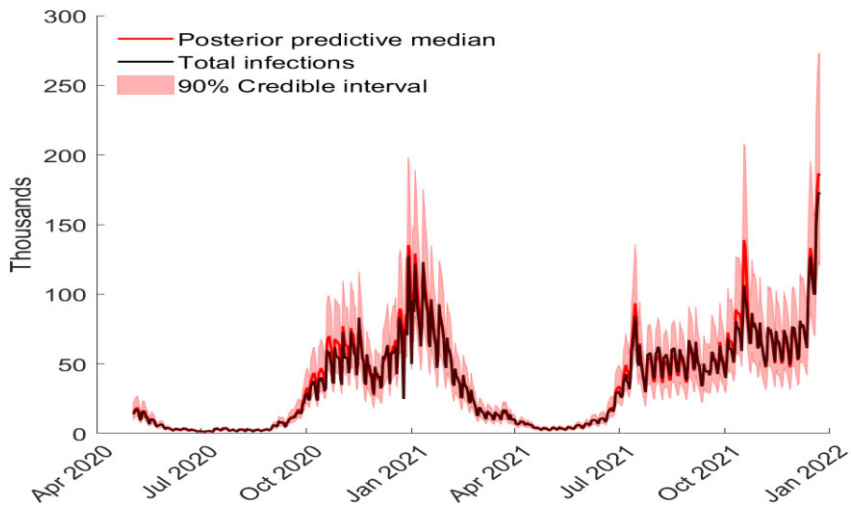

Figure 3. Fitted versus total cases.

The way the model is written may suggest that some parameters only enter multiplicatively and cannot be identified; however, the regimes over which these parameters are identified only partially overlap, and this is ensured by gluing the transition functions, allowing identification from the time variation in the nonoverlap periods. In the Online Appendix, Section S2, we show that the posteriors for most parameters are tighter than their priors, and further demonstrate

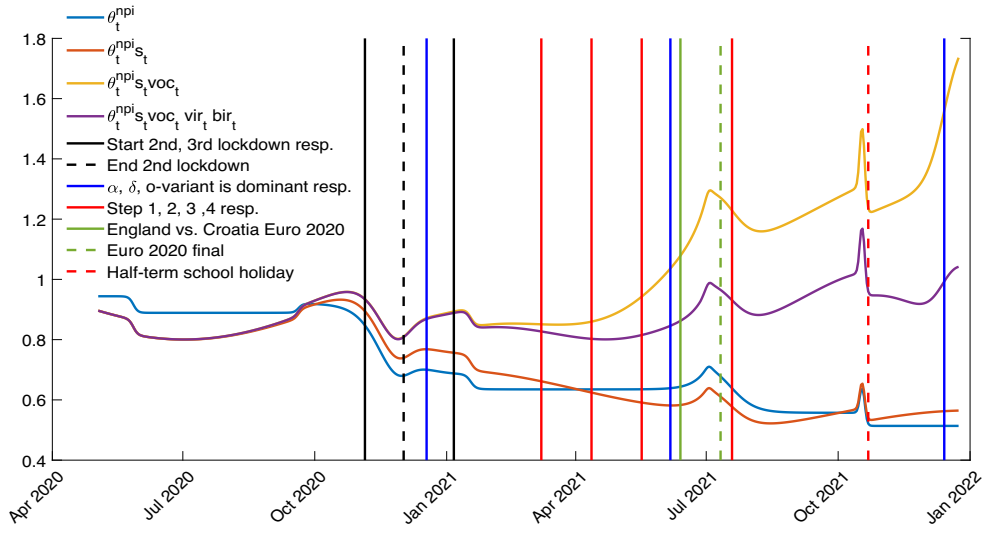

Figure 4. Estimated time evolution of posterior median estimates of the parameters associated with previous day infections y_{t-1}.

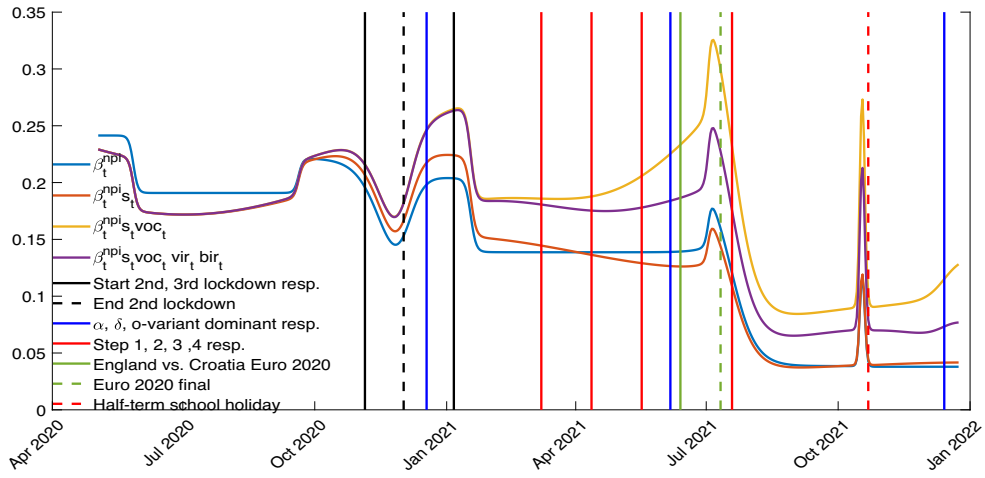

Figure 5. Estimated time evolution of posterior median estimates of the parameters associated with previous day intensity λ_{t-1}.

identification through simulations. The model implies that $E[\lambda_t|\mathcal{F}_{t-1}] = \bar{\theta}_t y_{t-1} + \bar{\beta}_t \lambda_{t-1}$, where $\bar{\theta}_t = \hat{\theta}_t^{\text{npi}}\, s_t\, \widehat{\text{voc}}_t\, \widehat{\text{vir}}_t\, \widehat{\text{bir}}_t$ and $\bar{\beta}_t = \hat{\beta}_t^{\text{npi}}\, s_t\, \widehat{\text{voc}}_t\, \widehat{\text{vir}}_t\, \widehat{\text{bir}}_t$. All parameters with 'hat' denote the posterior median from Table 3. All parameter functions with 'hat' are obtained by plugging in the posterior median of all estimated parameters from Table 3. In Figures 4 and 5, we plot $\bar{\theta}_t$ and $\bar{\beta}_t$ against vaccinations and the timing of various measures. In these figures, Steps 1–4 refer to

the steps in the roadmap out of the third lockdown (that took place in early 2021) in England. We further plot the contribution to the time evolution of $\bar{\theta}_t$ of the estimates $\hat{\theta}_t^{\text{npi}} s_t$ and $\hat{\theta}_t^{\text{npi}} s_t \widehat{\text{voc}}_t$, and similarly for $\bar{\beta}_t$. Figure 4 shows that, in principle, conditional on our model assumptions, and assuming these parameters do not only capture temporary protection from a previous infection, NPIs were effective should they have been implemented against the wild-type variant, but because of new variants their effectiveness dropped over time. The figure also shows that vaccines and boosters substantially mitigated this drop. We see a drop in $\bar{\theta}_t$ in the summer of 2020, followed by an increase in autumn 2020. This second wave seems to be brought under control by a second lockdown, but $\bar{\theta}_t$ starts to increase again as the Alpha variant takes over. At the same time, vaccinations begin and this tempers down the increase until the Delta variant takes over and large events such as the Euro-2020 cup (that took place in summer 2021) are allowed, in which period the transmission soars. With these events no longer in place, the transmission decreases again, but then schools open and we see another steep surge, which is tempered by school holidays, but most importantly by boosters being widely administered. We see a similar evolution for $\bar{\beta}_t$ in Figure 5, except that as the Omicron BA.1 variant becomes dominant (end of 2021), this parameter stays low. This can be explained by the fact that $\bar{\beta}_t$ measures intensity clustering, and with Omicron, because of immune escape from previous variants, a large share of the population gets infected quickly, and therefore the wave also dies off faster. Nevertheless, the estimate of $\bar{\beta}_t$ is not close to zero, indicating that this dependence is not negligible. This also motivates our use of the reinforcing term $\bar{\beta}_t \lambda_{t-1}$: without it, the dependence on infections on the recent past infections cannot be easily quantified.

3.3. Counterfactual analysis

We use the estimates from Subsection 3.2 to run counterfactuals regarding the timing and intensity of booster campaigns (Figure 6 and Figure S12 from Section S5 in the Online Appendix) and NPIs (Figure 7 and Figure S15 from Section S5 in the Online Appendix). In all figures, the shaded areas represent the interquartile range from 4,000 negative binomial draws (in the Online Appendix, Section S5, Figures S13–S14 and S16–S17, we included the same projections, but with the lower 5% to the upper 95% quantiles). In all figures, the projected daily infections (solid lines) are given by the median of these 4,000 draws. Recall that we denote with a hat all posterior median estimates from Table 3, which are then plugged in to obtain the estimates $\hat{\theta}_i$, $\hat{\beta}_i$, $\hat{f}_{i,s}$, $(i = 1, \ldots, 9)$ and the corresponding time-varying functions $\hat{\theta}_s^{\text{npi}}$, $\hat{\beta}_s^{\text{npi}}$, $\hat{g}_{j,s}$ $(j = \alpha, \delta, o, v, b)$, $\widehat{\text{voc}}_s$ in-sample: $s = 1, \ldots T$, and out-of-sample: $s = T + \ell, \ldots$, with $\ell > 1$. Similarly, $\widehat{\text{vir}}_s$ and $\widehat{\text{bir}}_s$ are the in-sample time evolution of the estimated functions $\text{vir}_s, \text{bir}_s$ for $s = 1, \ldots, T$. For $t = T + \ell$ $(\ell \geq 1)$, a draw from the negative binomial is:

$$\tilde{y}_t \sim \text{NegBinomial}(\tilde{\lambda}_t, \hat{\phi}), \tag{3.1}$$

and the parameters' time evolution for this draw are given by

$$\begin{aligned} &\tilde{\lambda}_{T+1}^{\text{npi}} = \hat{\theta}_{T+1}^{\text{npi}} y_T + \hat{\beta}_{T+1}^{\text{npi}} \hat{\lambda}_T^{\text{npi}}, \text{ and} \\ &\tilde{\lambda}_t = \tilde{\lambda}_t^{\text{npi}} \, s_t \, \widehat{\text{voc}}_t \, \widetilde{\text{vir}}_t \, \widetilde{\text{bir}}_t, \; \tilde{\lambda}_t^{\text{npi}} = \hat{\theta}_t^{\text{npi}} \tilde{y}_{t-1} + \hat{\beta}_t^{\text{npi}} \tilde{\lambda}_{t-1}^{\text{npi}}, \text{ for } t = T + \ell, \quad \ell \geq 2, \end{aligned} \tag{3.2}$$

where $\widetilde{\text{vir}}_t, \widetilde{\text{bir}}_t$ are defined below. Figure 6 shows a hypothetical scenario in which the booster campaign started as in reality, but the population is reached at different speeds and/or more people received the booster. In this counterfactual, $t = T + 1$ in (3.1) corresponds to 27 November 2021 (when the first case of Omicron BA.1 variant was identified in England). As one cannot have a

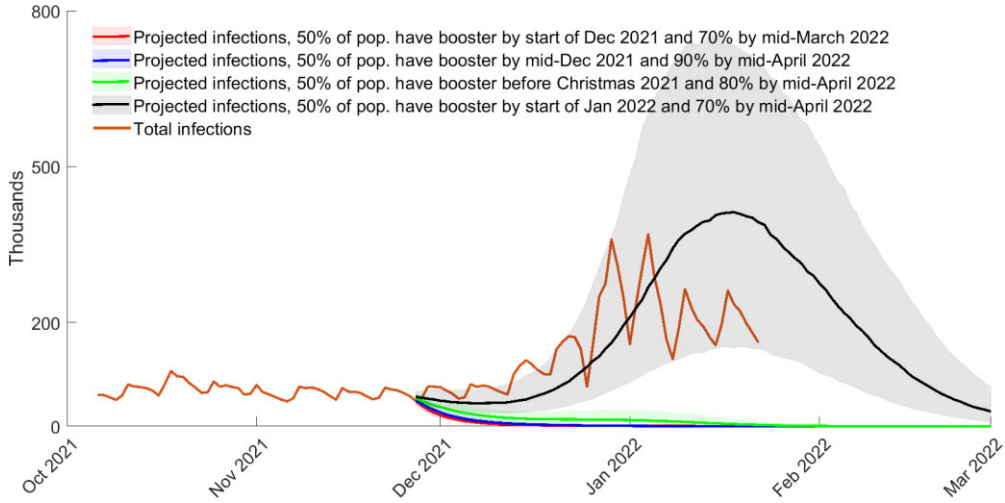

Figure 6. Counterfactual when the vaccine booster campaign starts on 16 September 2021 and population is reached at different speeds; projection of daily infections from 27 November 2021; bir $= 0.69$ (posterior median) and $\rho_o = 0.41$ (posterior median); booster wanes after five months.

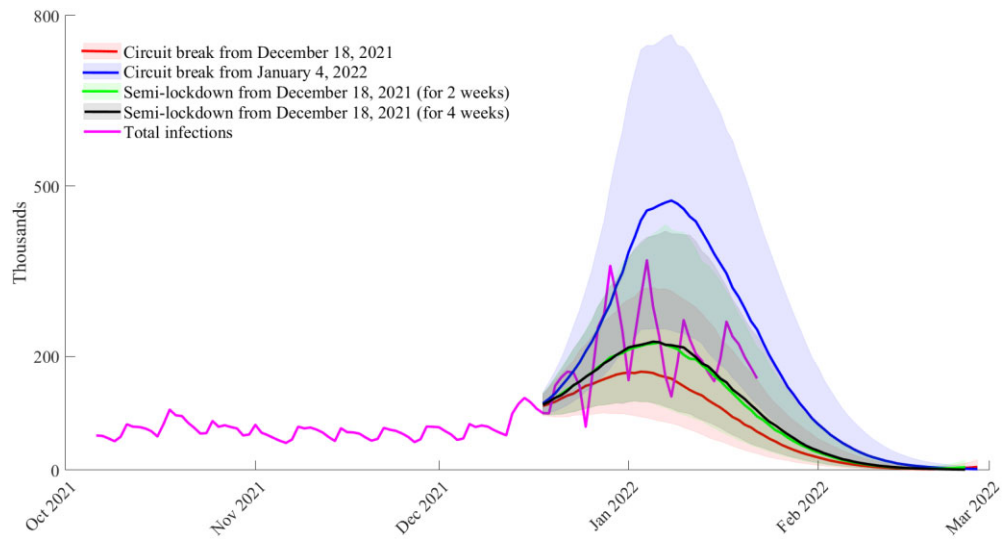

Figure 7. Counterfactual when there is a circuit break (two weeks hard lockdown) from 18 December 2021 or 4 January 2022 (peak of infections) or when there is a semi-lockdown from 18 December 2021 (for two weeks or four weeks); projection of daily infections from 18 December 2021; bir $= 0.69$ (posterior median) and $\rho_o = 0.41$ (posterior median); booster wanes after five months.

booster without being fully vaccinated first, for vaccines we use the transition function estimated from the vaccination data, but with total vaccinated population share $c \in \{0.7, 0.8, 0.9\}$, where $c = 0.7$ is what actually occurred, and $c > 0.7$ are hypothetical scenarios where the vaccination speed is faster. More exactly, in (3.2) we use:

$$\widetilde{\text{vir}}_t = (1 - \tilde{g}_{v,t}) + (1 - \widehat{\text{vir}}\, w_{v,t})\tilde{g}_{v,t}, \qquad \tilde{g}_{v,t} = \frac{c}{1 + \exp(-\hat{h}_v(t - \hat{t}_v^{\perp}))},$$

where the second dose vaccine waning, $w_{v,t}$, starts on 28 June 2021 (as considered in the estimation, Table 3), and $c = 0.7, 0.8, 0.9$. For the booster, we use:

$$\widetilde{\text{bir}}_t = (1 - \tilde{g}_{b,t}) + (1 - \widehat{\text{bir}}\, w_{b,t})\tilde{g}_{b,t}, \qquad \tilde{g}_{b,t} = \frac{c}{(1 + \exp(-\hat{h}_b(t - \tilde{t})))},$$

with $\tilde{t} = 14$ November 2021 and $c = 0.7$ (70% of the population is vaccinated). This scenario corresponds to the situation when 50% of the population is reached by the beginning of December 2021. The booster waning, $w_{b,t}$, starts five months after 16 September 2021. It is calculated as in (2.5) with $t^+ = 14$ February 2022. In Figure 6 we also consider the hypothetical scenario when 50% of the population is reached later in December 2021 and by the beginning of January 2022, in which case we take $\tilde{t} = 9$ December 2021 with different speeds: $c = 0.9$ (90% of the population is vaccinated), $c = 0.8$ (80% of the population is vaccinated), $c = 0.7$ (70% of the population is vaccinated). In Figure 6 we present the projected daily infections from 27 November 2021 (when the first case of Omicron BA.1 variant was identified in England). The results in Figure 6 suggest that the speed of the booster campaigns would have been key to maintain the spread of Omicron. The estimated model predicts that, had 50% of the population received a booster before Christmas 2021, then the winter wave driven by the spread of Omicron could have been avoided. If 50% of the population is boosted by early January (which is what occurred), then the estimated model predicts a winter wave similar to what was observed up to the start of 2022 with a peak being reached in mid-January 2022. In reality, the number of infections peaked in early January, which suggests that the measures adopted during December 2021 (after mid-December masks became mandatory in most public indoor venues, individuals were advised to work from home, and proof of vaccination was required to enter nightclubs or attend large gatherings) to contain the spread of Omicron may have had an impact (note that the projected daily median infections in the scenarios are considered to start on 27 November 2021, which is prior to the adoption of restriction measures in December 2021). Figure S12 from the Online Appendix, Section S5, suggests that if the booster campaign started one month earlier (in mid-August rather than mid-September 2021) and quickly reached a significant fraction of the population, the winter infection wave could have been avoided. However, it also suggests that an early start would not have been sufficient to avoid a winter wave if the booster uptake was not fast enough. The Online Appendix, Section S3, provides a discussion of the (limitations of giving) behavioural interpretations of our model and results.

Figure 7 presents a counterfactual analysis with a circuit breaker (two weeks of hard lockdown as recommended by one member of the Scientific Advisory Group for Emergencies in England) and a semi-lockdown (similar to what was implemented by the government in England after mid-December 2021). The projected daily infections are from 18 December 2021 ($t = T + 1$ in (3.1) corresponds to this date). In particular, $\widetilde{\text{vir}}_t = \widehat{\text{vir}}_t$ and $\widetilde{\text{bir}} = \widehat{\text{bir}}$ with booster waning function $w_{v,t}$ calculated as in (2.5) with $t^+ = 14$ February 2021 (waning starts five months after

mid-September 2021).[12] We consider the following hypothetical evolution of the parameters due to the NPIs:

$$\begin{aligned}\bar{\theta}_t^{\text{npi}} &= \hat{\theta}_0(1-\hat{f}_{1,t}) + \sum_{i=1}^{8}\hat{\theta}_i\hat{f}_{i,t}(1-\hat{f}_{i+1,t}) + \hat{\theta}_9\hat{f}_{9,t}(1-f_{10,t}) \\ &\quad + (\hat{\theta}_9 - 0.05)f_{10,t}(1-f_{11,t}) + (\hat{\theta}_9 - 0.05 + \hat{\gamma}_8)f_{11,t} \\ &\approx \hat{\theta}_9\hat{f}_{9,t}(1-f_{10,t}) + (\hat{\theta}_9 - 0.05)f_{10,t}(1-f_{11,t}) + (\hat{\theta}_9 - 0.05 + \hat{\gamma}_8)f_{11,t}, \quad (3.3)\end{aligned}$$

$$\begin{aligned}\bar{\beta}_t^{\text{npi}} &= \hat{\beta}_0(1-\hat{f}_{1,t}) + \sum_{i=1}^{8}\hat{\beta}_i\hat{f}_{i,t}(1-\hat{f}_{i+1,t}) + \hat{\beta}_9\hat{f}_{9,t}(1-f_{10,t}) \\ &\quad + (\hat{\beta}_9 - 0)f_{10,t}(1-f_{11,t}) + (\hat{\beta}_9 + \hat{\omega}_8)f_{11,t} \\ &\approx \hat{\beta}_9\hat{f}_{9,t}(1-f_{10,t}) + (\hat{\beta}_9 - 0)f_{10,t}(1-f_{11,t}) + (\hat{\beta}_9 + \hat{\omega}_8)f_{11,t}, \quad (3.4)\end{aligned}$$

where the approximations in (3.3) and (3.4) follow from the fact that for $t = T+1, \ldots$, the transition function $\hat{f}_{9,t}$ is the dominant one and the transition functions for the previous regimes have no impact. In (3.3) and (3.4) above, $f_{10,t}$ is the transition function from relaxation to hard lockdown or semi-lockdown:

$$f_{10,t} = \frac{1}{1+\exp(-k_{10}(t-t^*))},$$

with t^*= 22 December 2021 (for the circuit breaker starting on 18 December 2021), t^*= 8 January 2022 (for the circuit breaker starting on 4 January 2022 when total infections reach their peak), and t^*= 28 December 2021 (for the semi-lockdown that starts on 18 December 2021). We take $k_{10} = 0.1$ (similar to $\hat{k}_3$, the estimate of steepness of the transition function $\hat{f}_{3,t}$ from relaxation to hard lockdown in November 2020 in Table 3, therefore also assuming that protection from a previous infection, which is not explicitly modelled, but may be absorbed in the estimation of the NPI specific parameters, is the same as that embedded in estimation of $\hat{k}_3$). For the hard lockdown, the midpoint of the transition function is reached four days after the lockdown is imposed, while for the semi-lockdown the midpoint is reached after 10 days. Hence, the transition function is steeper for the hard lockdown compared to the semi-lockdown. The exit from lockdown in period with relaxation is captured through the transition function

$$f_{11,t} = \frac{1}{1+\exp(-k_{11}(t-t^-))},$$

with steepness equal to $k_{11} = 1$ ($\approx \hat{k}_8$ the steepness of the transition function $\hat{f}_{8,t}$ to a period of full relaxation in the summer and autumn 2021, see Table 3). Moreover, t^-= 20 February 2022 (for the circuit breaker on 18 December with exit in two weeks), t^-= 8 March 2022 (for the circuit breaker on 4 January with exit in two weeks), t^-= 10 March 2022 (for the semi-lockdown on 18 December with an exit in two weeks), t^-= 23 March 2022 (for the semi-lockdown on 18 December with an exit of four weeks). For all scenarios in Figure 7 we assume that the exit is in two or four weeks after the lockdown is imposed, but we allow for the fact that restrictions are usually lifted gradually, not in one go. To account for this, the midpoint of the transition function from lockdown to relaxation is reached 50 days after the measures are lifted. The choice of 50 days is motivated by the fact that

[12] The cases when booster waning starts earlier in $t^+ = 15$ January 2021 (four months after mid-September 2021) or later in $t^+ = 16$ March 2021 (six months after mid-September 2021) are presented in Online Appendix Figure S15.

between the midpoint of $\hat{f}_{7,t}$ and that of $\hat{f}_{8,t}$ (between the big sport event at the beginning of July 2021 and the peak of infections in late October 2021 when full relaxation measures were in place and the Delta variant was dominant) there are 90 days. The results from Figure 7 are similar if the midpoint of $f_{11,t}$ is reached after 100 days (if restrictions are lifted slower). As seen from (3.3), the parameter associated with previous day infections, y_{t-1}, transitions from $\hat{\theta}_9$ to $\hat{\theta}_9 - 0.05$ during lockdown (to reflect that the lockdown reduces the infections). The choice of 0.05 is similar to $\hat{\gamma}_5$ (see Table 3) in regime 5 (after the third lockdown that started in January 2021). As seen from (3.4), the parameter associated with past daily intensity λ_{t-1} remains unchanged. This is motivated by the fact that, starting with the period when Omicron became dominant, the importance of λ_{t-1} has diminished, while the importance of y_{t-1} in triggering new infections has increased, reflecting the fact that Omicron is more transmissible than previous variants, and evades previous temporary immunity from an infection with a previous variant. Once the lockdown ends, the parameters increase by $\hat{\gamma}_8$ and $\hat{\omega}_8$ (the posterior medians of the parameters associated with the NPI in the summer 2021 when full relaxation measures were in place) from Table 3.

Figure 7 suggests that the timing of adoption of restriction measures may be crucial. If a lockdown had been implemented in mid-December 2021 then the estimated model predicts that the increase in cases in early winter due to Omicron could have been mitigated. However, a late lockdown or a semi-lockdown of either two or four weeks would not have been as effective. Note that the semi-lockdown scenario of four weeks is close to what the government implemented (the government restrictions were put in place between mid-December to late January, approximately six weeks) and the estimated model projections track well the total realized daily cases out of sample. The similarity between the counterfactual cases of two and four weeks semi-lockdown indicates that perhaps the government could have ended restrictions earlier than it did and that would not have resulted in a significant increase in infections.

3.4. Scenarios

In this section, we provide scenarios for the evolution of total COVID-19 cases six months out of sample. As in Subsection 3.3, the shaded areas in all figures represent the interquartile range from 4,000 negative binomial draws (in the Online Appendix, Section S6, we included the same figures, but with the lower 5% to the upper 95% quantiles). The projected daily infections are given by the median from these 4,000 draws. The draws are obtained as described at the beginning of Subsection 3.3 and are based on (3.1)–(3.2), with $t = T + 1$ corresponding to 25 December 2021. Moreover,

$$\begin{aligned}\widetilde{\text{voc}}_t &= (1 - \hat{g}_{\alpha,t}) + (1 + \hat{\rho}_\alpha)\hat{g}_{\alpha,t}(1 - \hat{g}_{\delta,t}) + (1 + \hat{\rho}_\alpha)(1 + \hat{\rho}_\delta)\hat{g}_{\delta,t}(1 - \hat{g}_{o,t}) \\ &\quad + (1 + \hat{\rho}_\alpha)(1 + \hat{\rho}_\delta)(1 + \hat{\rho}_o)\hat{g}_{o,t}(1 - g_{BA.2,t}) \\ &\quad + (1 + \hat{\rho}_\alpha)(1 + \hat{\rho}_\delta)(1 + \hat{\rho}_o)(1 + \rho_{BA.2})g_{BA.2,t} \\ &\approx (1 + \hat{\rho}_\alpha)(1 + \hat{\rho}_\delta)(1 + \hat{\rho}_o)\,(1 - g_{BA.2,t} + (1 + \rho_{BA.2})g_{BA.2,t}), \qquad (3.5)\end{aligned}$$

where the approximation (3.5) follows from the fact that Omicron is dominant at the end of the sample; $\rho_{BA.2}$ is the intensity increase parameter for the Omicron BA.2 variant relative to the

Omicron BA.1 variant, and $g_{BA.2,t}$ is the transition function of the Omicron BA.2 variant

$$g_{BA.2,t} = \frac{1}{1+\exp(-\hat{\kappa}_o(t-t^{**}))},$$

with $\hat{\kappa}_o$ the steepness of the transition function for the Omicron BA.1 variant $\hat{g}_{o,t}$, and the mid-time of $g_{BA.2,t}$ is $t^{**} =$ 5 February 2022, that is 12 days after the first cases of infections with the Omicron BA.2 variant were genomically confirmed in England. For the Omicron BA.1 variant, the mid-time in the transition function was estimated to be 16 days after the first case appeared in England (27 November 2021). Thus, we assume that the BA.2 variant spreads more rapidly than the BA.1 variant. In obtaining the draws $\tilde{y}_t$, we imposed:

$$\begin{aligned}\bar{\theta}_t^{\text{npi}} &= \hat{\theta}_0(1-\hat{f}_{1,t}) + \sum_{i=1}^{8}\hat{\theta}_i\hat{f}_{i,t}(1-\hat{f}_{i+1,t}) + \hat{\theta}_9\hat{f}_{9,t}(1-f_{10,t}) + (\hat{\theta}_9+\hat{\gamma}_8)f_{10,t}\\ &\approx \hat{\theta}_9\hat{f}_{9,t}(1-f_{10,t}) + (\hat{\theta}_9+\hat{\gamma}_8)f_{10,t},\\ \bar{\beta}_t^{\text{npi}} &= \hat{\beta}_0(1-\hat{f}_{1,t}) + \sum_{i=1}^{8}\hat{\beta}_i\hat{f}_{i,t}(1-\hat{f}_{i+1,t}) + \hat{\beta}_9\hat{f}_{9,t}(1-f_{10,t}) + (\hat{\beta}_9+\hat{\omega}_8)f_{10,t}\\ &\approx \hat{\beta}_9\hat{f}_{9,t}(1-f_{10,t}) + (\hat{\beta}_9+\hat{\omega}_8)f_{10,t},\end{aligned}$$

where $f_{10,t}$ is the transition function from some relaxation measures to full relaxation

$$f_{10,t} = \frac{1}{1+\exp(-k_{10}(t-t^{***}))},$$

with $k_{10} = 1$ ($\approx \hat{k}_8$ the steepness of the transition function $\hat{f}_{8,t}$ to a period of full relaxation in the summer and autumn 2021, see Table 3). We consider two cases for t^{***}. The first one corresponds to a scenario with an early impact of measures lifted: $t^{***} =$ 13 March 2022 (50 days after 27 January 2021 when measures of Plan B were lifted).[13] The second case corresponds to a scenario with a late impact of measures lifted: $t^{***} =$ 6 May 2022 (100 days after 27 January 2021 when measures of Plan B were lifted). Finally, to obtain the draws $\tilde{y}_t$, we have $\widetilde{\text{vir}}_t = \widehat{\text{vir}}_t$ and

$$\widetilde{\text{bir}}_t = (1-\hat{g}_{b,t}) + (1-\widetilde{\text{bir}}\, w_{b,t})\hat{g}_{b,t},$$

where $\widetilde{\text{bir}} = 0.75$. We chose a higher bir because the scenarios with $\widetilde{\text{bir}} = \widehat{\text{bir}} = 0.69$ (the posterior median) seem pessimistic when plotted against infections in February 2022 (which were not used in the estimation, but just plotted out of sample). In Figure 8 we consider the scenario with a 10% relative intensity increase of the Omicron BA.2 variant ($\rho_{BA.2} = 10\%$) with the shared areas representing the interquartile range. In the Online Appendix, Section S6, we consider also $\rho_{BA.2} \in \{5\%, 20\%\}$ (Figures S18–S19). In Figure 8 and Figures S18–S19 (Section S6 of the Online Appendix) we assume that the booster wanes in five months, and the Online Appendix (Section S7, Figures S23–S25) shows the same scenarios, but with waning of the booster after six months. In all these figures, we consider projections when NPIs are not lifted, and lifted having an early impact or a late impact on infections. Black dots indicate the observed total daily cases and the black line the in-sample posterior medians from Section 2.

[13] Plan B refers to measures introduced on 8 December 2021, in England: working from home for those who can, face mask wearing to most public indoor venues, vaccine passport, and daily tests for those who are contacts of Omicron cases.

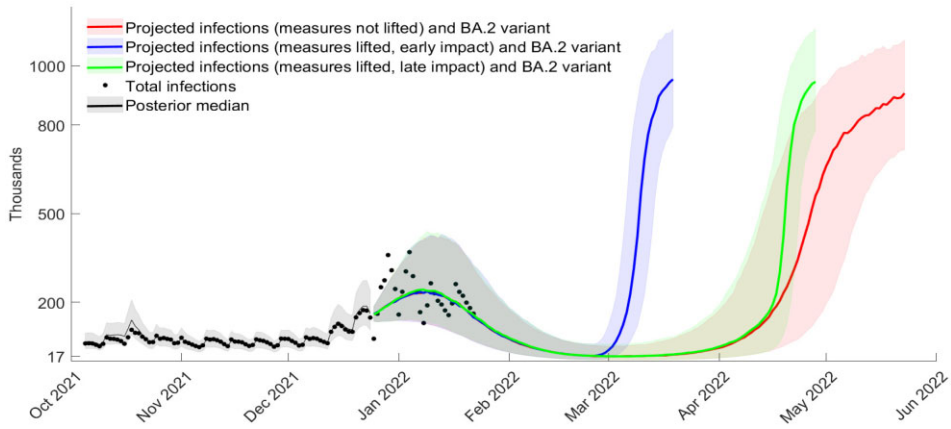

Figure 8. Projected total cases from 25 December 2021, waning of boosters after five months, bir $= 0.75$, $\rho_o = 0.41$ (posterior median), relative BA.2 intensity increase $\rho_{BA.2} = 10\%$; booster wanes after five months.

Figure 8 suggests that if there is a late impact from lifting the restrictions, or restrictions are not lifted, a new wave starts later, in mid-April 2022. If there is an early impact from lifting the restrictions, a wave starts in March. In reality, the ONS survey and UK dashboard data indicate that a large infection wave did occur in March, consistent with early impact of lifting restrictions. Since there is evidence that there were few reinfections with Omicron BA.2 after an infection with Omicron BA.1 around that time—Stegger et al. (2022)—this can be attributed largely to the government lifting restrictions and prevention measure, and the average individual taking advantage of the relaxation measures.[14]

4. CONCLUSION

We proposed a dynamic intensity model for SARS-CoV-2 infections in England to disentangle between NPIs, vaccines uptake, and variants of concern. We find that NPIs were effective at reducing infections in all waves so far, but that they worked best with the wild-type variant, which is natural, given the fact that more infectious variants are harder to contain. We also found that the decrease in effectiveness of the same NPIs due to more infectious variants was strongly mitigated by vaccines and boosters. Our counterfactuals suggest that, had the booster campaign started one month earlier, or if it had reached a significant fraction of the population faster, then the winter wave in December 2021 could have been avoided. We also show that a two-week lockdown implemented early would have been much more effective at reducing infections in December 2021 than the longer semi-lockdown actually implemented. Projections suggest that as booster protection wanes, another wave is predicted to occur. The predicted timing for the new wave is affected by several factors: (1) NPIs; (2) infectiousness of Omicron BA.2 variant; (3) timing for the waning of booster protection; and (4) efficacy of boosters at reducing infection

[14] The Online Appendix Section S8 also shows how to use our results to project ahead hospital admissions, which we find are still substantial in projected new waves.

intensity. While our scenarios are focused on Omicron BA.1 and BA.2, our framework can also be employed for new variants of concern, to inform policy makers about the necessity and timing of further booster campaigns and NPIs. Note that our analysis would not have been possible without using both daily reported cases and correcting for under-reporting using the ONS survey (Office for National Statistics, 2022c), which to our knowledge is unique due to high frequency testing of a large representative sample of the population. Other corrections, for example using available seroprevalence or sewage data, require much more modelling due to their indirect relationship to the number of cases, and are less reliable due to lower data frequency, waning, or weather patterns in the case of sewage. This highlights the importance of designing such surveys for other countries as well, and continually funding them, as long as the pandemic is not under control, to inform policy makers about the total number of cases. Knowing the total number of daily cases is important, not only for projecting future hospitalizations, but also for calculating expected long COVID cases, and the disruptions to society created by illness absences at school and work.

REFERENCES

Agosto, A. and P. Giudici (2020). A poisson autoregressive model to understand COVID-19 contagion dynamics. *Risks 8*, 1–8.

Arias, J. E., J. Fernández-Villaverde, J. F. Rubio-Ramírez and M. Shin (2023). The causal effects of lockdown policies on health and macroeconomic outcomes. Forthcoming in American Economic Journal: Macroeconomics. https://mcmcs.github.io/papers/covid_afrs_20220220.pdf.

Casey-Bryars, M., J. Griffin, C. McAloon, A. Byrne, J. Madden, D. Mc Evoy, Á. Collins, K. Hunt, A. Barber, F. Butler, E. A. Lane, K. O'Brien, P. Wall, K. Walsh and S. J. More (2021). Presymptomatic transmission of SARS-CoV-2 infection: a secondary analysis using published data. *BMJ Open 11*, e041240.

Fernández-Villaverde, J. and P. Guerrón-Quintana (2021). Estimating DSGE models: Recent advances and future challenges. *Annual Review of Economics 13*, 229–52.

Gelman, A., G. B. Carlin, H. S. Stern, D. B. Dunson, A. Vehtari and D. B. Rubin (2020). *Bayesian Data Analysis* (3rd ed.). Boca Raton: Chapman and Hall/CRC Texts in Statistical Science Series.

Giudici, P., B. Tarantino and A. Roy (2023). Bayesian time-varying autoregressive models of COVID-19 epidemics. *Biometrical Journal 65*(1). https://papers.ssrn.com/sol3/papers.cfm?abstract_id=3892996.

Götz, T., W. Bock, R. Rockenfeller and M. Schäfer (2021). A two-strain SARS-COV-2 model for Germany: Evidence from a linearization. ArXiv preprint. https://arxiv.org/abs/2102.11333.

Gourieroux, C. and J. Jasiak (2023). Time varying Markov process with partially observed aggregate data: An application to coronavirus. *Journal of Econometrics 232*(1), 35–51. https://doi.org/10.1016/j.jeconom.2020.09.007.

Hansen, P. R. (2022). Relative contagiousness of emerging virus variants: An analysis of the Alpha, Delta, and Omicron SARS-CoV-2 variants. *Econometrics Journal*, *25*(3), 739–61. https://academic.oup.com/ectj/advance-article/doi/10.1093/ectj/utac011/6553812.

Hortaçsu, A., J. Liu and T. Schwieg (2021). Estimating the fraction of unreported infections in epidemics with a known epicenter: An application to COVID-19. *Journal of Econometrics 220*, 106–29.

Jiang, F., Z. Zhao and X. Shao (2023). Time series analysis of COVID-19 infection curve: A change-point perspective. *Journal of Econometrics 232*(1), 1–17. https://doi.org/10.1016/j.jeconom.2020.07.039.

Keeling, M. J., A. Thomas, E. M. Hill, R. M. Thompson, L. Dyson, M. J. Tildesley and S. Moore (2021). Waning, boosting and a path to endemicity for SARS-CoV-2. MedRxiv preprint. https://www.medrxiv.org/content/10.1101/2021.11.05.21265977v2.

Khismatullina, M. and M. Vogt (2023). Nonparametric comparison of epidemic time trends: The case of COVID-19. *Journal of Econometrics 232*(1), 87–108. https://doi.org/10.1016/j.jeconom.2021.04.010.

Korolev, I. (2021). Identification and estimation of the SEIRD epidemic model for COVID-19. *Journal of Econometrics 220*, 63–85.

Lee, S., Y. Liao, M. H. Seo and Y. Shin (2021). Sparse HP filter: Finding kinks in the COVID-19 contact rate. *Journal of Econometrics 220*, 158–80.

Li, R., S. Pei, B. Chen, Y. Song, T. Zhang, W. Yang and J. Shaman (2020). Substantial undocumented infection facilitates the rapid dissemination of novel coronavirus (SARS-CoV-2). *Science 368*, 489–93.

Liu, L., H. R. Moon and F. Schorfheide (2021). Panel forecasts of country-level Covid-19 infections. *Journal of Econometrics 220*, 2–22.

Lloyd-Smith, J. O., S. J. Schreiber, P. E. Kopp and W. M. Getz (2005). Superspreading and the effect of individual variation on disease emergence. *Nature 438*, 355–59.

Neal, R. M. (2011). MCMC Using Hamiltonian dynamics. In S. Brooks, A. Gelman, G. L. Jones and X.-L. Meng (eds.), *Handbook of Markov Chain Monte Carlo*, pp. 113–62. Boca Raton: Chapman and Hall/CRC.

Office for National Statistics, (2022a). 'Coronavirus (COVID-19) Infection Survey: technical data'. https://www.ons.gov.uk/peoplepopulationandcommunity/healthandsocialcare/conditionsanddiseases URL/datasets/covid19infectionsurveytechnicaldata.

Office for National Statistics, (2022b). 'Coronavirus (COVID-19) Infection Survey: England'. https://www.ons.gov.uk/peoplepopulationandcommunity/healthandsocialcare/conditionsanddiseases URL/datasets/coronaviruscovid19infectionsurveydata/2022.

Office for National Statistics, (2022c). 'Coronavirus (COVID-19) Infection Survey: England'. https://www.ons.gov.uk/peoplepopulationandcommunity/healthandsocialcare/conditionsanddiseases URL/datasets/coronaviruscovid19infectionsurveydata/2022.

Pouwels, K. B., T. House, E. Pritchard, J. V. Robotham, P. J. Birrell, A. Gelman, K.-D. Vihta, N. Bowers, I. Boreham, H. Thomas, J. Lewis, I. Bell, J. I. Bell, J. N. Newton, J. Farrar, I. Diamond, P. Benton, A. S. Walker and the COVID-19 Infection Survey Team (2021). Community prevalence of SARS-CoV-2 in England from April to November, 2020: Results from the ONS Coronavirus Infection Survey. *Lancet Public Health 6*, e30–38.

Reynolds, C. J., C. Pade, J. M. Gibbons, A. D. Otter, K.-M. Lin, D. Mũnoz Sandoval, F. P. Pieper, D. K. Butler, S. Liu, G. Joy, N. Forooghi, T. A. Treibel, C. Manisty, J. C. Moon, Covidsortium Investigators, Covidsortium Immune Correlates Network, A. Semper, T. Brooks, Á. McKnight, D. M. Altmann and R. J. Boyton (2022). Immune boosting by B.1.1.529 (Omicron) depends on previous SARS-CoV-2 exposure. *Science 377*(6603). doi:10.1126/science.abq1841.

Roy, A. and S. Karmakar (2021). Time-varying auto-regressive models for count time-series. *Electronic Journal of Statistics 15*, 2905–38.

Rozhnova, G., C. H. van Dorp, P. Bruijning-Verhagen, M. C. J. Bootsma, J. H. H. M. van de Wijgert, M. J. M. Bonten and M. E. Kretzschmar (2021). Model-based evaluation of school- and non-school-related measures to control the COVID-19 pandemic. *Nature Communications 12*, 1614.

Sonabend, R., L. K. Whittles, N. Imai, P. N. Perez-Guzman, E. S. Knock, T. Rawson, K. A. M. Gaythorpe, B. A. Djaafara, W. Hinsley, R. G. FitzJohn, J. A. Lees, D. T. Kanapram, E. M. Volz, A. C. Ghani, N. M. Ferguson, M. Baguelin and A. Cori (2021). Non-pharmaceutical interventions, vaccination, and the SARS-CoV-2 delta variant in England: A mathematical modelling study. *Lancet 37*, 1825–35.

Stegger, M., S. M. Edslev, R. N. Sieber, A. C. Ingham, K. L. Ng, M.-H. E. Tang, S. Alexandersen, J. Fonager, R. Legarth, M. Utko, B. Wilkowski, V. Gunalan, M. Bennedbæk, J. Byberg-Grauholm, C. Holten Møller, L. E. Christiansen, C. W. Svarrer, K. Ellegaard, S. Baig, T. B. Johannesen, L. Espenhain, R. Skov, A. S. Cohen, N. B. Larsen, K. M. Sørensen, E. D. White, T. Lillebaek, H. Ullum, T. Grove Krause, A. Fomsgaard, S. Ethelberg and M. Rasmussen (2022). Occurrence and significance of Omicron BA.1 infection followed by BA.2 reinfection. *MedRXiv.* https://www.medrxiv.org/content/10.1101/2022.02.19.22271112v1.

Toulis, P. (2021). Estimation of Covid-19 prevalence from serology tests: A partial identification approach. *Journal of Econometrics 220*, 193–213.

UK Health Security Agency (2022). 'UK Coronavirus Dashboard'. https://coronavirus.data.gov.uk/details/download.

Viana, J., C. H. van Dorp, A. Nunes, M. C. Gomes, M. van Boven, M. E. Kretzschmar, M. Veldhoen and G. Rozhnova (2021). Controlling the pandemic during the SARS-CoV-2 vaccination rollout. *Nature Communications 12*, 3674.

Wearing, H. J., P. Rohani and M. J. Keeling (2005). Appropriate models for the management of infectious diseases. *PLoS Medicine 2*, 7.

SUPPORTING INFORMATION

Additional Supporting Information may be found in the online version of this article at the publisher's website:

Online Appendix
Replication Package

Co-editor Victor Chernozhukov handled this manuscript.